Open access wind tunnel measurements of a downwind free yawing wind turbine

Verelst, DRS; Larsen, TJ; van Wingerden, Jan-Willem

DOI
10.1088/1742-6596/753/7/072013

Publication date
2016

Document Version
Final published version

Published in
Journal of Physics: Conference Series

Open Access Wind Tunnel Measurements of a Downwind Free Yawing Wind Turbine

2016 J. Phys.: Conf. Ser. 753 072013

(http://iopscience.iop.org/1742-6596/753/7/072013)

Open Access Wind Tunnel Measurements of a Downwind Free Yawing Wind Turbine

[1] David Verelst, [1] Torben Larsen and [2] Jan-Willem van Wingerden

[1] DTU Wind Energy - Loads and Control, [2] TU Delft - Delft Center for Systems and Control

E-mail: dave@dtu.dk

Abstract. A series of free yawing wind tunnel experiments was held in the Open Jet Facility (OJF) of the TU Delft. The ≈ 300 W turbine has three blades in a downwind configuration and is optionally free to yaw. Different 1.6m diameter rotor configurations are tested such as blade flexibility and sweep. This paper gives a brief overview of the measurement setup and challenges, and continues with presenting some key results. This wind tunnel campaign has shown that a three bladed downwind wind turbine can operate in a stable fashion under a minimal yaw error. Finally, a description of how to obtain this open access dataset, including the post-processing scripts and procedures, is made available via a publicly accessible website.

1. Introduction

The main focus of this publication is to present global performance parameters (thrust, free yaw response and indicative mechanical power/torque estimates) of results from a wind turbine measurement campaign of a free yawing downwind 3 bladed wind turbine (≈ 300 W, 1.6m rotor diameter). These results are published as an open access data set, and this paper intents to serve as its formally peer reviewed reference. The wind tunnel measurements were completed within the context of a PhD research project [1], and some of the preliminary results have been discussed earlier in comparison with aeroelastic simulations [2]. This paper further complements the earlier publications with additional free yawing results and indicative power/torque estimates. However, the presented work is not complete and not all issues concerning the presented data set are resolved.

Previous rotating wind tunnel experiments with at least a partial focus on yawed inflow conditions have been discussed in for example: [3], [4], [5], [6], [7], [8], [9], [10], [11], [12]. Although [5] considers a downwind rotor design, it does not explore the free yawing concept. These are an extensive set of measurement campaigns regarding yawed inflow conditions. However, to the author knowledges there are no other existing experiments that have studied the yaw stability of three bladed downwind free yawing wind turbine.

A 3 bladed free yawing downwind wind turbine could potentially reduce the yaw drive torque requirements, minimize its wear, maintenance, and hence ultimately reduce its costs. Assuming such a free yawing system can operate in a stable fashion and under minimal yaw error, it might also reduce average operating yaw errors compared to actively controlled yaw systems. In doing so the turbine loading could decrease while power output can be increased. Active yaw controllers have slow response times (in the order of minutes) and are based on low accuracy wind direction measurements (often installed on the nacelle directly behind the rotor). However, the

	region	t/c	Re_{design}	Re_{data}	$C_{L_{max}}$
NREL S823	inboard	21%	$4e5$	$1e5$	1.184
NREL S822	outboard	16%	$6e5$	$2e5$	1.100

Table 1. Blade airfoils and corresponding key parameters.

blade tower shadow passage of a downwind wind turbine introduces a challenge due to increased blade fatigue loading and reduced power output.

An alternative application of a good understanding of wind turbine performance and loading under yawed inflow could be to help predict more precisely the wind direction [13]. Considering this is often problematic when using only aerodynamic devices placed on the nacelle, a reliable method to determine the yaw error based on turbine loading and/or performance parameters can be valuable.

2. Experimental Setup and Limitations

The experiment consisted out of two campaigns: the first took place during February of 2012, and the second two months later in April 2012. A comprehensive discussion of the design of the experimental setup and measurement sensors are given in sections 4.4, 4.5 and 5.2 of [1]. What follows is a brief overview:

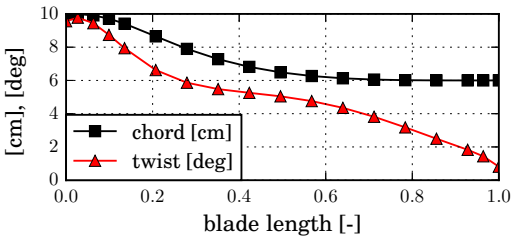

Figure 1. Rotor aerodynamic design.

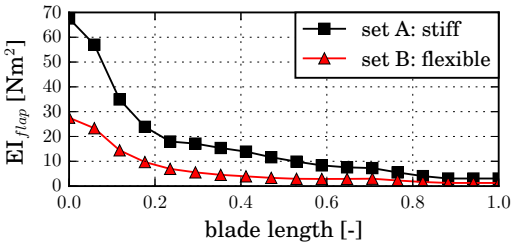

Figure 2. Estimated blade flapwise stiffness distribution.

- Rotor aerodynamic performance (ignoring flexibility): 280 W at 450 RPM and 11.4 m/s, $C_{P_{max}} = 0.36$ at TSR=6 (tip speed ratio).
- Rotor diameter: 1.60m, blade root radius : 0.245m, blade length=0.555m.
- The tower base is suspended on two bearings, allowing the complete tower to yaw. The nacelle is fixed to the tower top.
- Blades are made from PVC foam, optionally reinforced with glass fibre sandwich beam. Various rotor configurations have been considered (but all share the same aerofoil, and twist, chord length, and aerofoil thickness distributions, see figure 1):
  - Blade aerofoils: NREL S823 and S822 [14] (see table 1). Aerodynamic characteristics are taken from the UIUC LSAT database [15].
  - All blades are made from liquid PVC foam that was poured into a negative glass fibre mould. Some blades had an additional glass fibre sandwich core. Surface roughness was very smooth, expect for a higher roughness area along the leading edge ($\approx$ 1 mm wide).

  - Blade set A "stiff": 8-layered glass fibre sandwich core beam, strain gauges in flapwise direction (glued on core beam), flapwise stiffness derived from measured blade deflection curves with static tip load (see figure 2).
  - Blade set B "flexible": 2-layered glass fibre sandwich core beam, strain gauges in flapwise direction (glued on core beam), flapwise stiffness derived from measured blade deflection curves with static tip load (see figure 2).
  - Blade set C "flexible-no-beam": only PVC foam and no strain gauges, stiffness not quantified.
  - Blade set D "flexible-no-beam-sweep": swept planform, only PVC foam and no strain gauges, stiffness not quantified.
- In free yawing mode the yaw angle range is approximately -35 to 35 degrees. The yaw angle can be locked or manually controlled in free yaw mode from the control room using a system of simple ropes and pulleys.
- Positive values for the yaw angle ψ mean that blade moving upwards is closer to the wind. Alternatively, the yaw axis rotation vector is pointing down (vertically), and the rotor axis rotation vector is pointing into the wind (meaning the rotor is rotating "the wrong way").
- The generator is connected to a high and low electrical resistance dump load for limited torque variability (there is no active rotor speed control). The effective dump load magnitude is controlled by encoding a given set point with pulse width modulation (very fast switching between either dump loads). The low resistance is fully active for a duty cycle (dc) of 1, and the high resistance for a duty cycle value of 0. Any value in between can be considered as an interpolation between the high and low resistance dump load.
- Main measurement channels:
  - Electrical power dissipated in the dump load.
  - Rotor speed and azimuth angle measurement device.
  - Strain gauges on the tower base in for-aft and side-side directions.
  - Strain gauges on two blades of set A "stiff" and set B "flexible" in flapwise direction.
  - Laser distance meter to measure the yaw angle.

The limitations of the experiment are summarised as follows:

- Reliable measurement of the mechanical shaft power is missing.
- No yaw moment measurement device.
- Blade flap-wise strain gauge measurements are not reliable and significantly affected by centrifugal forces.
- Smaller blade deflections than aimed for due to higher than expected blade mass and PVC foam stiffness. This means
- Mass imbalances, especially for blade sets A "stiff" and B "flexible".
- Not so accurate pitch settings (± 1 deg), small pitch and cone angle imbalance.
- The results from the February campaign are largely unusable due to corrupted tower strain calibration measurements, low quality rotor speed measurements, low generator torque range and lacking generator data sheet (generator was upgraded in April).
- No accurate aerodynamic performance characteristics of the rotor (3D-correct lift, drag and moment coefficients).

However, the missing shaft torque/power measurement can be compensated to a certain extent by considering the measured torque-rpm-power characteristics provided by the generator manufacturer. This is discussed in more detail in the following sections.

3. Measurement Results

3.1. Overview

An overall overview of the test cases can be obtained by considering figures 3 and 4. From figure 3 the two operating modes of the turbine are clearly illustrated: low tip speed ratios when the rotor is operating in deep stall, and higher tip speed ratios (around the design point) in attached flow regimes.

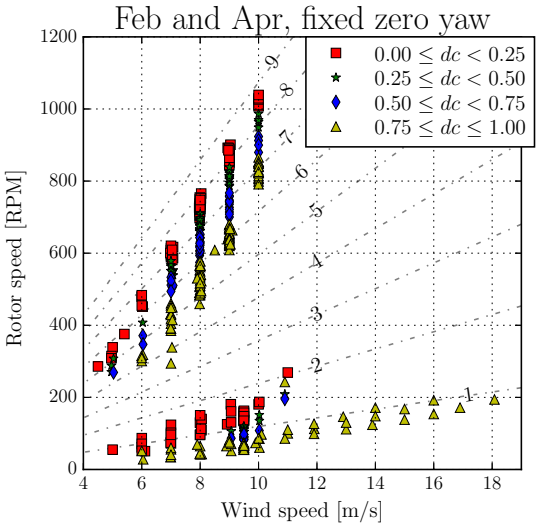

Figure 3. Rotor speed as function of wind speed in aligned flow for various generator load settings (dc). Dotted lines indicate tip speed ratios.

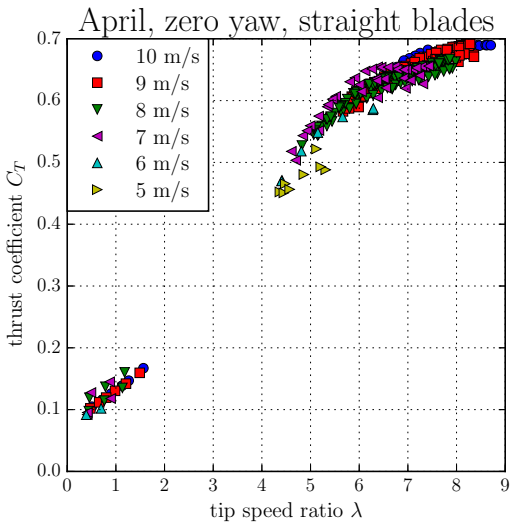

Figure 4. Thrust coefficients as function of tip speed ratio in aligned flow for various wind speeds.

The influence of yaw inflow angle on the rotor thrust is given for different tip speed ratios in figures 5 and 6 for the straight and swept blades respectively. The dash line indicated in both figures show that there is an indicative $cos^2\psi$ (with ψ being the yaw error) relationship between thrust and yaw angle. Further, a small skew in figures 5 and 6 is noted: the thrust coefficient has a slight asymmetry. For negative yaw errors the C_T is slightly higher compared to positive ones. Although there are less data points available for the swept blade, these results indicate they perform similarly. A definitive explanation for this asymmetry remains to be formulated. Possible causes could be due to tower shadow effects, misalignments in thrust measurements (which are based on for-aft and side-side strain gauges), or hypothetical non uniform artefacts in the wind tunnel velocity distribution. Investigation this further is referred to future work.

3.2. Estimating Rotor Mechanical Power

The mechanical and electrical performance of the generator have been documented by the manufacturer in the form of a rotor speed vs input torque, electrical current and voltage, and are given for a range of generator load resistance values in figure 7. The contour lines in figure 7 indicate regions for which the resistance is constant, and the labels indicate the magnitude of this resistance ranging from 28Ω (units Ohm, in dark red) to 4Ω (units Ohm, in dark blue). The corresponding generator efficiency is given in figure 8. Note that the efficiency only exceeds 56% for rotor speeds above 400 RPM.

The measurement data given in figures 7 and 8 is provided by generator manufacturer windbluepower.com and is re-used with their permission.

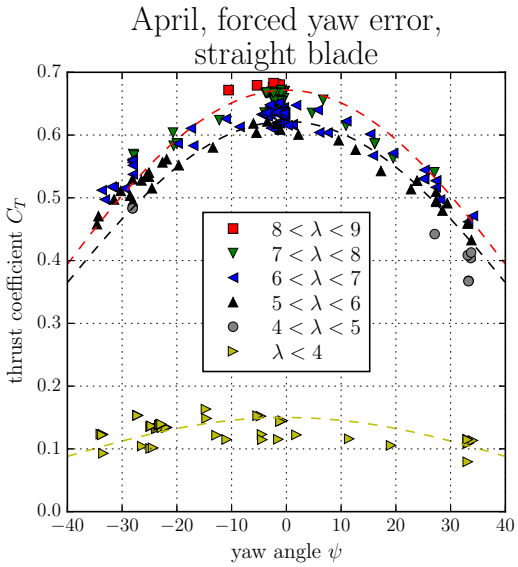

Figure 5. Thrust coefficients as function of yaw angle for various tip speed ratios and straight blades (sets A and B). Dashed lines are proportional to $cos^2\psi$ and are the same as in figure 6 to facilitate visual inspection.

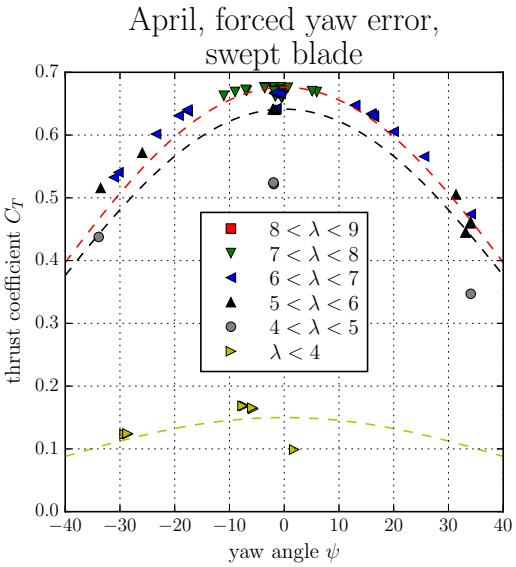

Figure 6. Thrust coefficients as function of yaw angle for various tip speed ratios and swept blades (set D). Dashed lines are proportional to $cos^2\psi$ and are the same as in figure 5 to facilitate visual inspection.

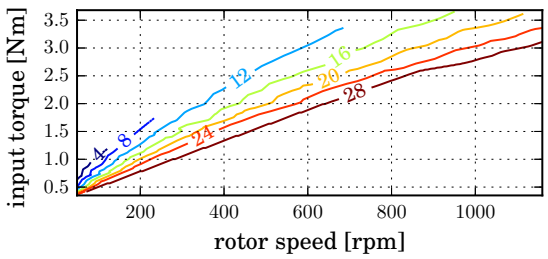

Figure 7. Measured applied torque and rotor speed for various electrical load settings (contour labels units are in Ohm).

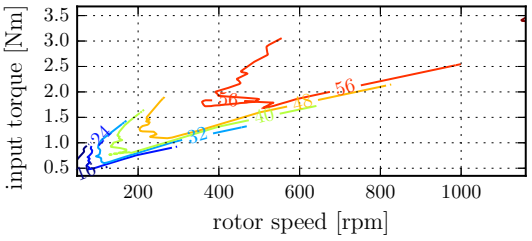

Figure 8. Measured generator electrical efficiency for a range of applied torque and rotor speeds at various electrical load settings (contour labels in %).

Although the effective generator load resistance was not determined accurately for the experimental setup, an estimate is available: 11Ω ([Ohm]) for duty cycle dc=1, and 28Ω for dc=0. Based on this data set, the generator electrical efficiency, mechanical torque and electrical power can be estimated by simply using the data of figure 7 as a lookup table: at a given generator speed and dump load magnitude (given by the duty cycle value) the mechanical torque can be found. The rotor speed measurement can now be used to estimate the rotor mechanical power and the generator electrical power. Note that due to a limited range of rotor speed data points in the generator measurement sheet provided by the manufacturer, not all wind tunnel measurement points have a corresponding estimated mechanical/electrical power value.

A comparison between the measured electrical power dissipated in the dump load and the estimated mechanical power (based on manufacturer data sheet) is given in figures 9 and 10

respectively. Both the measured and the estimated values correspond in order of magnitude. However, significant differences are noted:

- Measured electrical power (figure 9) seems to indicate a parabolic dependency on rotor speed, where the peak power nearly approaches the estimated mechanical power values as given in figure 10. This indicates that significant electrical losses occur elsewhere in the system, which can be confirmed by considering figure 8 that shows rapidly decreasing efficiency with decreasing rotor speed (or decreasing TSR at a given wind speed).
- Figure 11 shows that the measured electrical power rapidly drops for duty cycles approaching 1 (low resistance dump load setting). The corresponding mechanical power estimates in figure 12 show only a modest decrease in power when approaching duty cycle settings of 1.
- An more accurate and in detailed account of these electrical power measurements and corresponding estimated mechanical values is referred to future work.

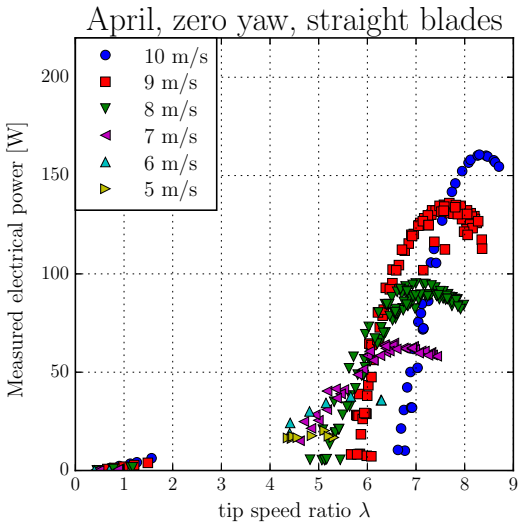

Figure 9. Measured electrical power as function of tip speed ratio in aligned flow for various wind speeds. Blade sets A and B.

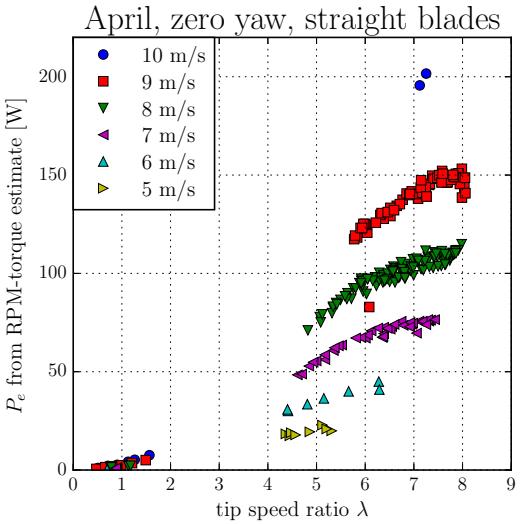

Figure 10. Generator electrical power based on RPM-torque data provided by manufacturer, using estimate for resistance value of dump load. Blade sets A and B.

Assuming that these estimate generator characteristics are somewhat sensible, the rotor power coefficient C_P (based on the estimated mechanical power) can be considered as function of TSR and yaw error in figures 13 and 14. However, figure 13 seems to indicate that the power coefficient has a Reynolds number dependency, while previously the thrust coefficients in figure 4 did not. Due to several possible sources of errors in the power estimation scheme considered here, it is likely that the dump load resistance estimates are inaccurate. It is suggested that a more detailed consideration and modelling of the electrical system is required (including pulse width modulation dump load switch) to increase the reliability of the mechanical power estimate. For example, the measured generator efficiency (figure 8) could be used to improve the effective generator dump load magnitude. The latter is also affected by power dissipated in the pulse width modulation system (which required active cooling using a fan and aluminium cooling block when operating at duty cycles other than 0 and 1) and the wiring between the generator and the dump load. However, these losses were not quantified during the experiment.

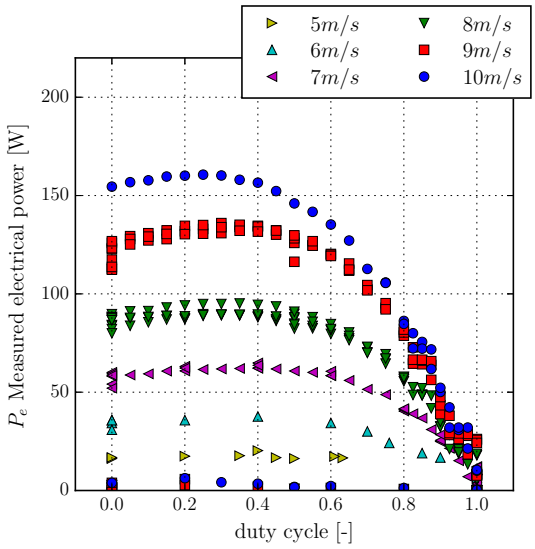

Figure 11. Measured electrical power as function of generator dump load resistance magnitude. Blade sets A and B.

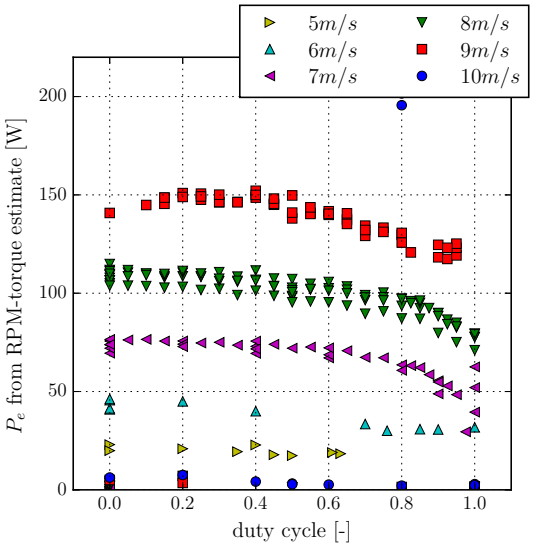

Figure 12. Generator electrical power (based on RPM-torque estimates) as function of generator dump load magnitude.

Due to the inaccuracies related with the estimated C_P, figure 14 is only included here as an indicative measure of yaw error on power coefficient. However, it is interesting to note that a similar (unexplained) asymmetry with respect to yaw error is observed compared to the thrust coefficients (figure 5): negative yaw errors result in slightly higher power coefficients.

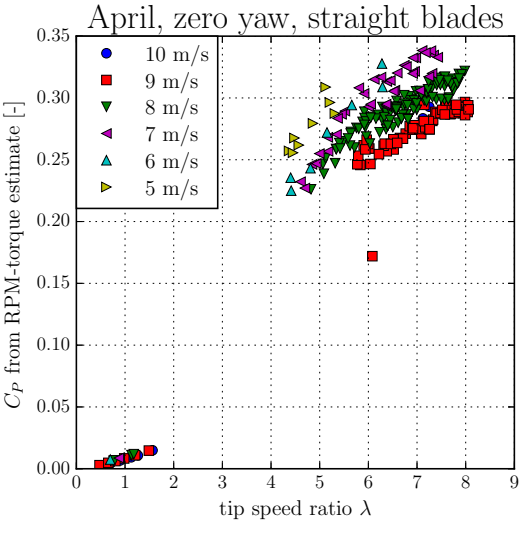

Figure 13. Estimated power coefficients as function of tip speed ratio in aligned flow for various wind speeds. Blade sets A and B.

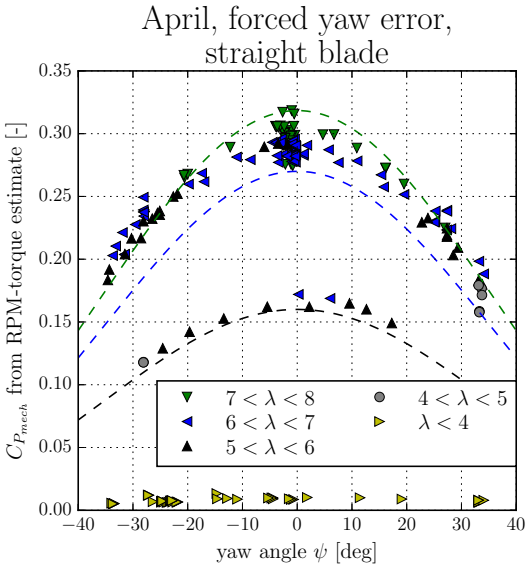

Figure 14. Estimated power coefficients as function of yaw angle for various tip speed ratios and straight blades. Dashed lines are proportional to $cos^3\psi$. Blade sets A and B.

3.3. Free yaw response

For the free yawing tests, the turbine was forced into a yaw error and released again after reaching steady rotor speed conditions. An example of such a result is given in figure 15: the rotor speed and yaw inflow angle are given for two different blade planform layouts: straight (blade sets A and B) and swept (blade set D). It is interesting to note that the yaw response is either under- or critically-damped. The rotor speed response is always critically- or over-damped. The largest contributing factor for the type of yaw response (critically- or under-damped) depends on the operating tip speed ratio, initial yaw error (both magnitude and sign). It is assumed this is due to the yaw moment dependency of rotor speed, wind speed and yaw inflow angle. A quantitative comparison between the performance of the free yaw response of the swept (set D) and straight blades (set A or B) would require the same initial conditions for both rotor speed and yaw angle. Unfortunately, such a combination is not available in the current data set.

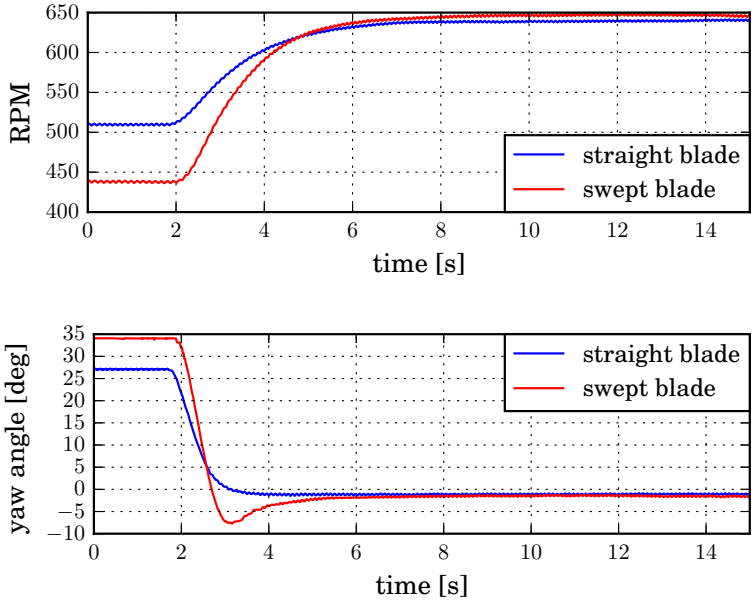

Figure 15. Comparison of a typical free yaw response of a straight and flexible blade at 9 m/s. Note the overshoot of the swept blade (set D) is assumed to be due to the higher initial yaw error and consequently higher initial yawing moment.

A series of these free yaw response experiments were recorded at various wind and rotor speeds, but unfortunately not at exactly the same initial yaw error and rotor speed. This makes a direct comparison difficult, as can be seen from figures 16 and 17 showing the respective rotor speed and yaw angle time traces. Figures 16-19 indicate:

- red for positive initial yaw errors
- blue for negative initial yaw errors
- triangles refer to the swept blades
- lines refer to straight blades
- figure 17 has a reversed left y-axis (yaw)

Note that for positive yaw errors the blade is moving upwards when rotated into the wind.

In order to perform a qualitative comparison between the different free yaw responses, and in an attempt to establish if there is a dependency on blade sweep (blade set D), the free yaw response rotor speed and yaw angles are normalized in figures 18 and 19.

The normalized rotor speed response (figure 18) seems roughly independent of blade type and initial yaw error. This indicates that the rotor torque changes due yaw misalignment are qualitatively speaking similar cases presented here.

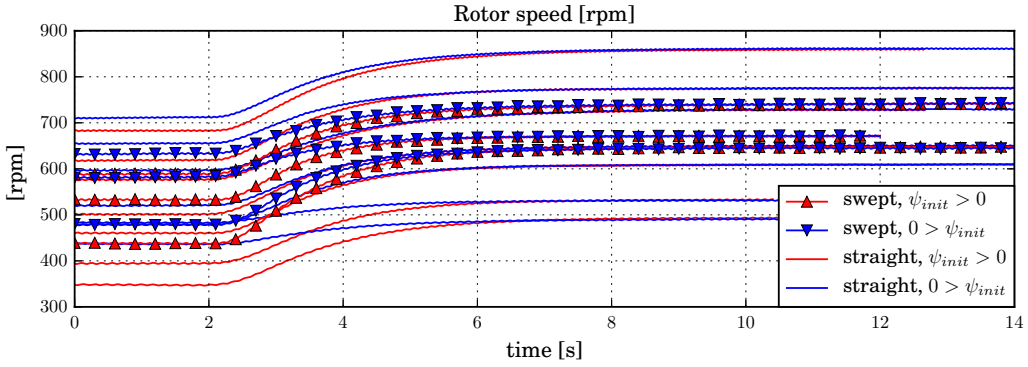

Figure 16. Free yaw response: rotor speed [rpm]. Red marks positive initial yaw errors, blue negative. Series indicated with a triangle refer to the swept blades, lines to straight blades.

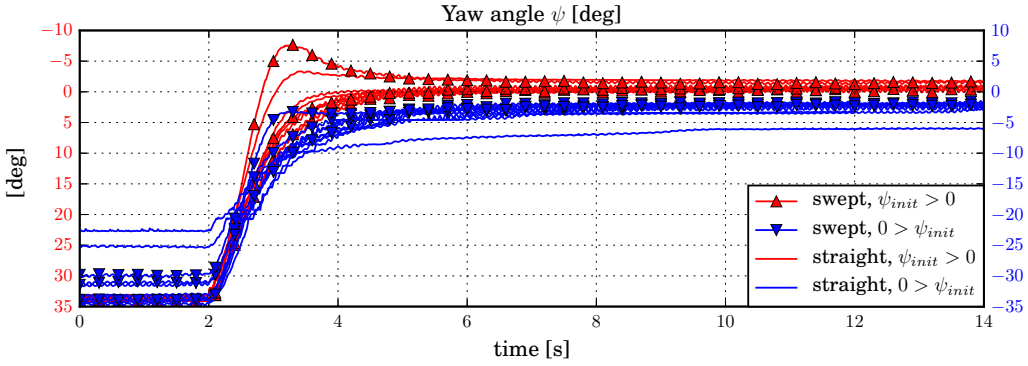

Figure 17. Free yaw response: yaw angle [deg]. Red marks positive initial yaw errors, blue negative. Series indicated with a triangle refer to the swept blades, lines to straight blades. Left y-axis is reversed compared to right y-axis.

When considering the yaw angle response (figures 17 and 19) the following observations are made:

- The steady state yaw angle is not exactly zero, and depends on the initial yaw error (figure 17). It is possible that the yaw inertia and bearing friction is of similar magnitude and therefore the steady yaw angle gets "stuck" in a region of low yawing moments. Detailed yaw moment measurements and/or simulations are required to further investigate this issue.
- Negative initial yaw errors result in a marginally higher steady state yaw angles (figure 17). A simple explanation could be that there is very small error on the yaw alignment. Alternatively, the tower shadow could have a contribution towards an asymmetric yaw inflow vs yaw moment distribution, and possibly a non zero yaw angle for zero yawing moment.
- A qualitative indication of the yaw stiffness is derived based on the slope of the free yaw response. Yaw stiffness for negative yaw errors seems to be lower compared to positive ones. Corresponding to the higher yaw stiffness, only positive yaw errors demonstrate an under-damped response for some cases.

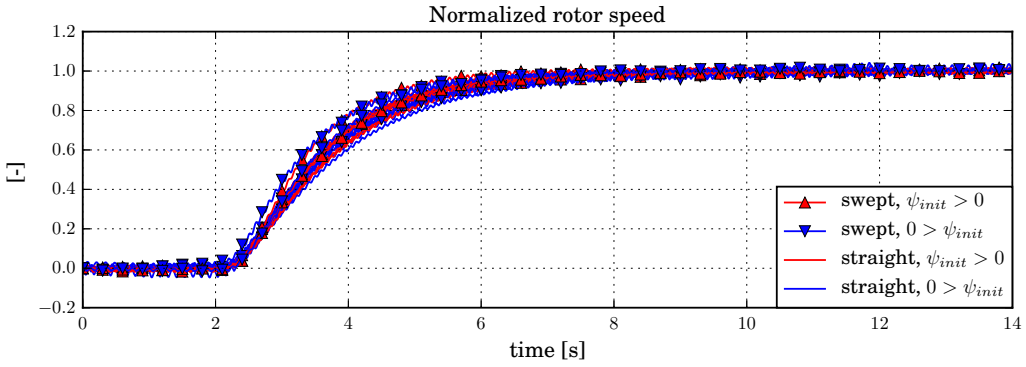

Figure 18. Normalized free yaw response: rotor speed.

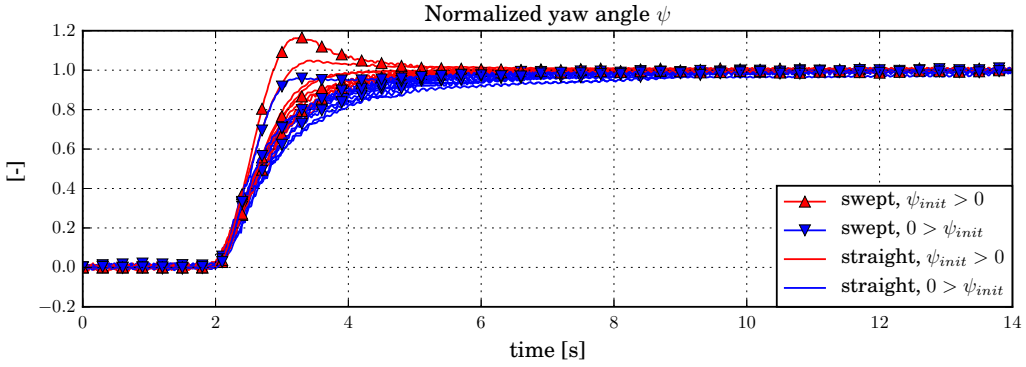

Figure 19. Normalized free yaw response: yaw angle.

4. Open Access Measurement Data

The underlying data set of this paper is open access and can be freely downloaded:

- Python post-processing callibration methods, plotting scripts, and representative aeroelastic beam model in HAWC2 format [16]. This serves at the main access points and includes further instructions on how to access the measurement data and contains descriptions on the data formats used.
- Measurement results (raw and calibrated), figures and plots of the results, pictures and video's of the experiment [17]
- LaTeXsources and figures for this paper [18]

This paper only presents a part of the available measurements, and the interested reader is referred to the given websites for more results.

5. Future Work, Recommendations Future Experiments

The estimated mechanical power results are not sufficiently accurate, and some suggestions were made that could help to improve it. Further, the slightly higher thrust coefficients at negative yaw errors need to be considered in more detail.

The current results have not been compared in detail with other yawed inflow experiments reported in literature, and this should be considered in future discussions in order to verify or refute conclusions drawn based on the this data set.

Some of the drawbacks of this experiment, such as missing accurate aerodynamic performance characteristics of the rotor (lift, drag and moment coefficients), can be mitigated by considering a large number of operating conditions. For example, in [19] the aerodynamic rotor characteristics are determined based on a large number of measurements with varying tip speed ratios and blade pitch angles. This requires careful planning of the experiment upfront the measurement campaign.

Fixed rotor speed control is essential when trying to cover a broad range of operating conditions. In doing so, it would be possible to test a larger range of tip speed ratios at various yawed inflow angles, and ideally also at various blade pitch angle settings.

When using a simple direct drive generator without active control, the outcome of the experiment would benefit from its accurate characterisation. Not only the torque-rpm-electrical power characteristics, but also the performance under various electrical loads, and the dynamic response.

So far the presence of a yawing wind turbine in the wind tunnel is assumed to not have any effect on the inflow conditions. Since the considered wind tunnel has an open measurement section, wall and blocking effects have been assumed to be insignificant. A more detailed aerodynamic investigation is required in order to verify that claim, but this is considered out of the scope here.

Finally, the yaw stability could be studied in more detail if a combination of various free yaw responses is combined with fixed yaw moment measurements, and a quantification of the yaw bearing friction moment.

6. Conclusions

This paper presented a short overview of some of the key results of a wind tunnel campaign of a free yawing down wind turbine, and illustrated that it can operate in a steady fashion under minimal yaw error in a free yawing configuration. Thrust and estimated power coefficients at various tip speed ratios have been presented for various yaw angles. However, the estimated mechanical power is not sufficiently accurate and a more detailed model of the electrical system has to be considered in order to improve it. In yawed inflow conditions the thrust is proportional to $cos^2\psi$, and a small asymmetry is observed resulting in slightly higher thrust values for negative yaw errors compared to positive ones is noted, but a definitive explanation is not given. In free yaw the turbine operates in a stable fashion, and the system has typically a critically-damped response when released from a larger (30-25 degrees) yaw error. Instructions are provided in order to download this open access data set.

References

[1] Verelst D R 2013 *Numerical and Experimental Results of a Passive Free Yawing Downwind Wind Turbine* Ph.D. thesis DTU Wind Energy URL `http://orbit.dtu.dk/files/59650574/DTU_Wind_Energy_PhD_0023_EN_.pdf`

[2] Verelst D R, Larsen T J and van Wingerden J W 2014 *Journal of Physics: Conference Series* URL `http://dx.doi.org/10.1088/1742-6596/555/1/012103`

[3] Haans W, Sant T, van Kuik G and van Bussel G 2005 *Journal of Solar Energy Engineering* **127** 456–463 ISSN 0199-6231 00034 URL `http://dx.doi.org/10.1115/1.2037092`

[4] Haans W, Sant T, van Kuik G and van Bussel G 2005 Measurement and Modelling of Tip Vortex Paths in the Wake of a HAWT Under Yawed Flow Conditions (American Institute of Aeronautics and Astronautics) ISBN 978-1-62410-064-2 00018 URL `http://arc.aiaa.org/doi/10.2514/6.2005-590`

[5] Bracchi T 2014 *Downwind Rotor: Studies on yaw Stability and Design of a Suitable Thin Airfoil* PhD NTNU 00000 URL `http://www.diva-portal.org/smash/record.jsf?pid=diva2%3A735581&dswid=-2798`

[6] Schepers J 2012 *Engineering models in wind energy aerodynamics: Development, implementation and analysis using dedicated aerodynamic measurements* PhD TU Delft URL `http://dx.doi.org/10.4233/uuid:92123c07-cc12-4945-973f-103bd744ec87`

[7] Schepers J, Boorsma K, Cho T, Gomez-Iradi S, Schaffarczyk P, Jeromin A, Shen W, Lutz T, Meister K, Stoevesandt B, Schreck S, Micallef D, Pereira R, Sant T, Madsen H and Sorensen N 2012 Final report of IEA Task 29, Mexnext (Phase 1): Analysis of Mexico wind tunnel measurements Tech. Rep. ECN-E–12-004 ECN URL http://www.ecn.nl/publications/ECN-E--12-004
[8] Mexnext IEA Wind Task 29 Mexnext URL http://www.mexnext.org/
[9] Schepers J and Snel H 2007 Model Experiments in Controlled Conditions Tech. Rep. ECN-E–07-042 ECN URL http://www.ecn.nl/publications/ECN-E--07-042
[10] Hand M M, Simms D A, Fingersh L J, Jager D W, Cotrell J R, Schreck S and Larwood S M 2001 Unsteady Aerodynamics Experiment Phase VI: Wind Tunnel Test Configurations and Available Data Campaigns Tech. rep. URL http://www.osti.gov/bridge/servlets/purl/15000240-1FhaHo/native/
[11] Loland K M 2011 *Wind Turbine in Yawed Operation* MSc NTNU URL http://ntnu.diva-portal.org/smash/record.jsf?pid=diva2:438671
[12] Haans W 2011 *Wind turbine aerodynamics in yaw: unravelling the measured rotor wake* PhD TU Delft URL http://resolver.tudelft.nl/uuid:57f0cea4-4e05-47bf-8f53-fb1d6e36d39f
[13] Bottasso C L and Riboldi C E D 2015 *Renewable Energy* URL http://dx.doi.org/10.1016/j.renene.2014.07.048
[14] Somers D 2005 The S822 and S823 airfoils Tech. Rep. NREL/SR-500-36342 NREL URL https://wind.nrel.gov/airfoils/Documents/S822,S823_Design.pdf
[15] Selig M, Lyon C, Giguère P, Ninham C and Guglielmo J 1996 Summary of low-speed airfoil data Tech. rep. URL http://www.ae.illinois.edu/m-selig/uiuc_lsat/Low-Speed-Airfoil-Data-V2.pdf
[16] Post-processing scripts, download instructions, data format descriptions. https://github.com/davidovitch/freeyaw-ojf-wt-tests
[17] Measurement results, figures, pictures and video's. https://data.deic.dk/shared/62ffdf2d57c8a0133a7f3a43671d0e23
[18] Torque paper latex souces. https://github.com/davidovitch/torque2016-freeyaw-measurements/
[19] Bottasso C L, Cacciola S and Iriarte X 2014 *Journal of Wind Engineering and Industrial Aerodynamics* **124** 29–45 ISSN 0167-6105 URL http://www.sciencedirect.com/science/article/pii/S0167610513002493